Rectification in donor–acceptor molecular junctions

2008 J. Phys.: Condens. Matter 20 374106

(http://iopscience.iop.org/0953-8984/20/37/374106)

J. Phys.: Condens. Matter **20** (2008) 374106 (8pp) doi:10.1088/0953-8984/20/37/374106

Rectification in donor–acceptor molecular junctions

M J Ford[1], **R C Hoft, A M McDonagh and M B Cortie**

Institute for Nanoscale Technology, University of Technology, Sydney, PO Box 123, Broadway, NSW 2007, Australia

E-mail: mike.ford@uts.edu.au

Received 14 February 2008, in final form 1 May 2008
Published 26 August 2008
Online at stacks.iop.org/JPhysCM/20/374106

Abstract

We perform density functional theory (DFT) calculations on molecular junctions consisting of a single molecule between two Au(111) electrodes. The molecules consist of an alkane or aryl bridge connecting acceptor, donor or thiol endgroups in various combinations. The molecular geometries are optimized and wavefunctions and eigenstates of the junction calculated using the DFT method, and then the electron transport properties for the junction are calculated within the non-equilibrium Green's function (NEGF) formalism. The current–voltage or $i(V)$ characteristics for the various molecules are then compared. Rectification is observed for these molecules, particularly for the donor–bridge–acceptor case where the bridge is an alkane, with rectification being in the same direction as the original findings of Aviram and Ratner (1974 *Chem. Phys. Lett.* **29** 277–83), at least for relatively large negative and positive applied bias. However, at smaller bias rectification is in the opposite direction and is attributed to the lowest unoccupied orbital associated with the acceptor group.

(Some figures in this article are in colour only in the electronic version)

1. Introduction

The idea that a single molecule can act as a current rectifier dates back to at least 1974. Aviram and Ratner [1] proposed a model for electron transport through a molecule connected to external reservoirs that predicts rectifying behaviour by a certain class of molecules, consisting of donor and acceptor groups separated by an insulating σ-bridge, the so-called DσA molecules. Electrons can tunnel effectively through the σ-barrier from the acceptor to donor groups, once a sufficient bias is applied to allow donation from the cathode to acceptor and donor to anode. Tunnelling in the opposite direction, however, is suppressed, giving the rectifying behaviour.

Experimental verification of this idea was slow to follow, due to a lack of tools to probe single-molecule transport. Early attempts [2] were questionable due to the uncertainty in the source of the rectification. Metzger [3] presented further experimental results, where the DσA molecular junction was formed from a Langmuir–Blodgett multi- or monolayer with a second electrode deposited onto the L–B layer. The molecule was γ-(n-hexadecyl)quinolinum tricyanoquinodimethanide. Substantial rectifying behaviour for the molecular junction was evident in the results with an asymmetry in the $i(V)$ curve of several orders of magnitude between forward and reverse bias.

In the intervening years there has been a wealth of further experimental and computational studies of molecular junctions and many aspects of the problem have been revealed (see, for example, [4–7] and references therein) such as the importance of the contact regions between molecule and electrode.

Nevertheless, computational attempts to directly verify the rectification are scarce or ambiguous. The calculations of Stokbro *et al* [8] for the DσA molecule of Ellenbogen and Lowe [9] showed little or no rectifying behaviour. The calculations did show that a resonant state delocalized across the molecule can form at particular applied bias due to states normally localized on the D and A portions of the molecule coming into alignment. No asymmetry was observed in the $i(V)$ curve because this effect is symmetric under a reversal of the bias polarity and because transmission coefficients at the resonances are small. The calculations were performed within the density functional theory–non-equilibrium Green's function method (DFT-NEGF). This method, despite some fundamental objections, has gained considerable prominence

[1] Author to whom any correspondence should be addressed.

Table 1. Orbital confinement radii (Bohr) for the atomic species corresponding to confinement energies of 5 and 0.5 mRyd.

		Confinement radius	
Atom	Orbital	5 mRyd	0.5 mRyd
Au	6s	7.2	9.1
	5d	5.1	6.7
C	2s	4.9	6.1
	2p	6.1	7.8
N	2s	4.3	5.4
	2p	5.4	6.9
O	2s	3.8	4.8
	2p	4.8	6.2
S	3s	4.8	5.9
	3p	6.1	7.6
H	1s	5.8	7.6

in first principles electron transport calculations and has provided considerable insight into factors that govern this transport [10].

The efficacy of Aviram–Ratner type molecules to rectify is an important question given that the whole molecular electronics paradigm is largely based upon their original proposal, but the extent to which such a technology might be viable remains unresolved. We have already shown [11] using a simple tunnel-barrier model that there may be a fundamental limit to the rectification possible from a molecular junction, and that this limit is relatively severe, with rectification ratios of no more than about 20 seeming possible. In this paper we test this predicted limit by performing rigorous calculations of the $i(V)$ characteristics of molecular junctions consisting of Au(111) electrodes and a conceptually simple, yet synthetically accessible, DσA molecule, 1-dimethylamino-4-nitrobutane. We assess the effect of the σ tunnel-barrier length by replacing the butane bridge with octane and the effect of reducing the height of this tunnel barrier by replacing it with a substituted benzene ring. The effects of replacing the donor or acceptor ends of the molecule with thiol linkers are also explored. The calculations are performed with the first principles DFT-NEGF formalism.

2. Method

Prior to performing transport calculations, the junction geometries are optimized using the SIESTA package [12, 13], an atomic basis set implementation of density functional theory [14, 15]. This is a periodic boundary conditions code with basis sets represented by a linear combination of numerical atom-centred functions. In the present calculations we are using the Perdew–Burke–Ernzerhof (PBE) [16] formulation of the generalized gradient approximation to the exchange–correlation functional.

Double-ζ plus polarization functions are included in the basis for the valence orbitals of each atom. The basis functions have finite spatial extent, going strictly to zero outside a user-defined radius. The confinement radii for each angular momentum component of each atomic species are defined by a common 'energy shift' parameter, $\delta\varepsilon$, which specifies the increase in energy of the orbital resulting from this confinement. This parameter can be particularly critical to surface calculations where it is necessary for the wavefunction to extend into the vacuum beyond the surface. Plane-wave basis set calculations are often perceived as superior in this regard: however, from our previous work we know that reliable structures and interaction energies for adsorbates can be obtained at reasonable confinement radii [17], but properties such as work functions require considerably more extended orbitals [18]. Consequently, for the structure calculations this parameter is set to 5 mRyd, while for the transport calculations, the basis set size is reduced to single-ζ plus polarization orbitals on the Au atoms and the confinement is reduced, $\delta\varepsilon = 0.5$ mRyd. We have previously shown that reducing the confinement is more pertinent to obtaining converged transport properties than using a larger basis set [19]. The confinement radii resulting from these values of $\delta\varepsilon$ are listed in table 1.

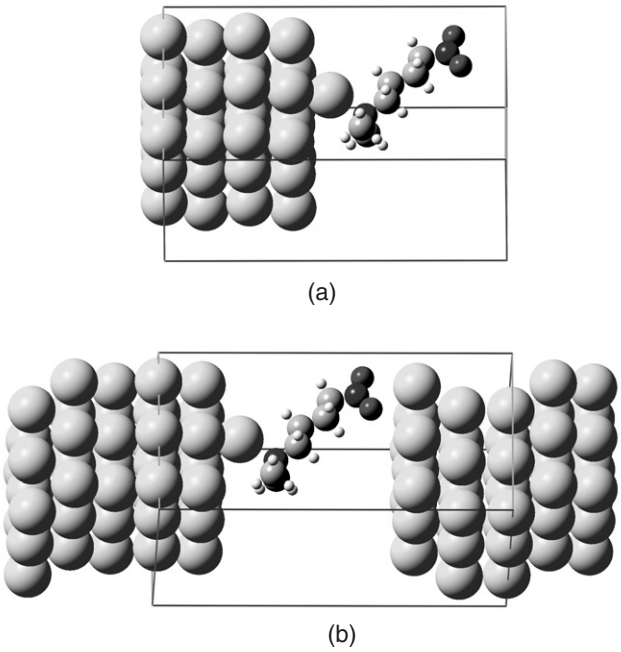

Figure 1. (a) SIESTA unit cell and (b) TranSIESTA-C unit cell for the calculations on 1-dimethylamino-4-nitrobutane (D–C_4H_8–A).

Each ion plus its core electrons are described by norm-conserving pseudo-potentials, constructed according to the scheme proposed by Troullier and Martins [20]. The electron density is represented on a real-space grid with spacings defined by the highest energy plane wave that can be represented on the grid without aliasing. This parameter is set to 200 Ryd and increased to 300 Ryd in the transport calculations.

The unit cell for the geometry optimization calculations is shown in figure 1(a). The molecules are placed on an Au(111) surface consisting of four layers with 3×3 Au atoms per layer in the unit cell. This provides sufficient spacing between the molecule and its periodic images to avoid intermolecular interactions. The unit cell length normal to the slab (z direction) is set so there is a 2 Å space to the right of the molecule. Because of the periodic boundary conditions of the calculation this means the right-hand end of

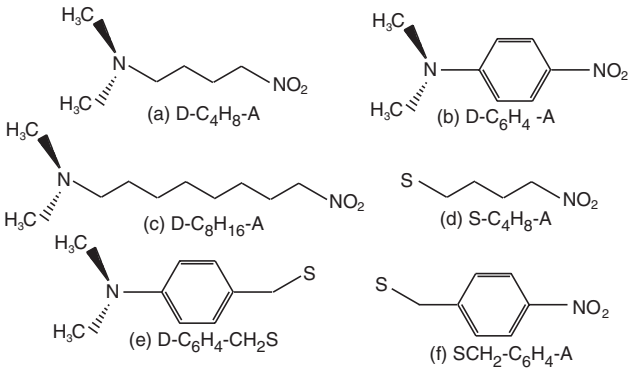

Figure 2. Molecules used in the Au(111)–X–Au(111) junction; (a) 1-dimethylamino-4-nitrobutane (D–C_4H_6–A), (b) 1-dimethylamino-4-nitrophenylene (D–C_6H_4–A), (c) 1-dimethylamino-4-nitro-octane (D–C_8H_{16}–A), (d) nitrobutanethiol (S–C_4H_8–A), (e) 1-dimethylamino-4-methanethiolphenylene (D–C_6H_4–CH_2S) and (f) nitrophenylmethanethiol (SCH_2–C_6H_4–A).

the molecule is sited 2 Å from the periodic image of the slab, that is, the molecule is sandwiched between two electrodes. A four-layer slab is the minimum thickness that can realistically be used without incurring significant interaction through the slab. All atoms in the unit cell are allowed to relax using a modified Broyden scheme [21]. The geometry is considered optimized once all Cartesian force components are below 0.04 eV $Å^{-1}$. Although this is a relatively modest tolerance for the optimization, improving the force convergence does not change the minimum energy structure substantially and consequently it does not change the $i(V)$ characteristic. The stress on the unit cell is calculated and the unit cell vectors allowed to relax accordingly.

In figure 1 an Au adatom is present between the surface and adsorbed molecule. In this case the molecule is D-butane-A, the donor is a dimethylamino group and the acceptor a nitro group. It is important to note the orientation of the molecule relative to the electrodes with the donor group attached to the left electrode and acceptor to the right electrode; this is reversed relative to the original Aviram and Ratner configuration. The molecule is bound to the surface through the nitrogen atom of the donor and the Au adatom. In previous work we have found that addition of an adatom yields a far greater interaction energy, by a factor of two, than adsorption onto a flat surface [22]. Recent conductance measurements of amine molecules bound to a gold surface suggest that the atop site is the most likely binding configuration [23]. The same donor and acceptor groups are used in all cases, and an adatom geometry is used for all molecules containing both the donor and acceptor. In cases where the donor or acceptor are replaced by a methane–thiolate group no adatom is present and the S atom is bound directly to the usual near-bridge site [24]. The molecules employed in this study are shown in figure 2. In each case the molecule is oriented relative to the electrodes as shown in this figure, with the donor group attached to the left electrode and the acceptor to the right.

During the geometry optimizations, reciprocal space is sampled on a grid of 3 × 3 k-points in the plane of the surface, constructed according to the method of Monkhorst and Pack [25]. No sampling is done in the direction normal to the slab. Due to software restrictions, the transport calculations are performed with the Γ-point only. We have previously found that, while this may not result in accurate absolute current values, the trends observed at higher sampling are preserved [19]. The separate calculation of the bulk electronic structure of the electrodes is done with 100 k-points in the direction of transport.

Transport calculations are performed on the relaxed junction geometries using the TranSIESTA package [26]. This uses the SIESTA method to obtain the electronic structure and then calculates transport properties by using the non-equilibrium Green's function method. The code has now been used extensively in the literature, for example, other studies have been undertaken to investigate the effect of different bonding geometries of small organic molecules between gold electrodes on the current–voltage characteristics of the system [27–29].

The device region (see figure 1(b)) consists of the molecule with two slab layers on either end, taken from the optimized unit cell of figure 1(a). This is coupled to bulk Au electrodes on the left and right. The non-equilibrium Green's function technique is used to calculate the transmission function between the electrodes. Separate calculations on the bulk electrodes provide the self-energies required to obtain the device Green's function. Finally the current is evaluated from Landauer's formula. The self-consistent calculation for each junction is repeated for different bias voltages, $-3.0\ \mathrm{V} \leqslant V \leqslant 3.0\ \mathrm{V}$, in steps of 0.2 V. For consistency with our previous work, a positive current/voltage corresponds to electron transport from the left to right electrode in the junction; this is the opposite convention to that used in TranSIESTA but the same as that used in the Aviram and Ratner paper. Remember, however, we have oriented the acceptor and donor groups of our molecule in the opposite direction to Aviram and Ratner. A positive bias is therefore where a positive potential is applied to the right electrode.

3. Results and discussion

The $i(V)$ characteristics were calculated for the six representative molecules shown in figure 2. Each consists of either an alkane chain or a substituted benzene ring with endgroups chosen from a sulfur atom, methylsulfide group, nitro group or dimethylamino group. The sulfur atom (S) or methanethiol group ($-CH_2S$) provides a strong bond to the electrode. The nitro group (A) serves as an electron acceptor while the dimethylamino group (D) serves as an electron donor. The junction $i(V)$ curves for each molecule are shown in figure 3. Each junction is constructed as in figure 1 by replacing 1-dimethylamino-4-nitrobutane with the appropriate molecule.

In this paper we describe the process of electron transport in these molecular junctions by the term 'tunnelling' even though the calculated currents are perhaps large (μA) compared with those expected in a traditional barrier tunnelling process (nA). Resonant tunnelling, charge transfer or other

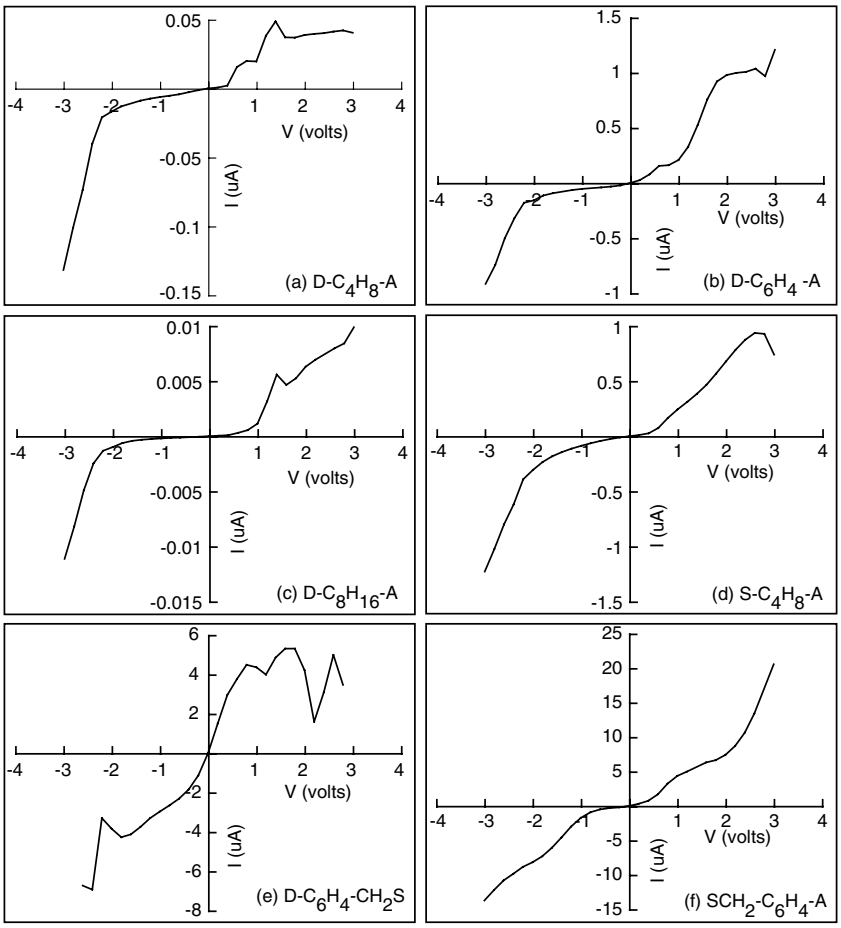

Figure 3. $i(V)$ curves for the six molecules shown in figure 2.

terms might be more accurate descriptions: however, for simplicity we will use the single term 'tunnelling'.

Figures 3(a)–(c) show similar qualitative $i(V)$ characteristics for the three donor–acceptor molecules. In the negative quadrant, the calculated current increases quite rapidly at a bias of about -2.5 V. For forward bias regions in figures 3(a)–(c), the positive quadrants of the $i(V)$ curves show a number of features. The current initially increases more rapidly with applied bias compared to the negative bias quadrant and thus the curves are asymmetric with respect to the forward and reverse directions. This is most evident in the case of the D–C_4H_8–A molecule (figure 3(a)) and less pronounced for the longer alkane bridge (D–C_8H_{16}–A) and even less so for the aryl bridge (D–C_6H_4–A). Doubling the length of the alkane bridge from butane (figure 3(a)) to octane (figure 3(c)) decreases the current at any given bias by an order of magnitude. Introduction of the substituted benzene ring as a bridging group between the donor and acceptor endgroups (figure 3(b)) increases the current by over an order of magnitude compared to the D–C_4H_8–A molecule (figure 3(a)).

In figures 3(d)–(f), either the donor or acceptor endgroup is replaced by a thiol linkage to the gold electrode. The terminal hydrogen on the sulfur atom has been removed and the sulfur forms a strong bond with the gold surface atoms. The effect of this replacement is to increase the current by an order of magnitude compared to the corresponding donor–acceptor molecules. The $i(V)$ curves where the donor group has been replaced in the alkane and aryl bridged molecules is considerably smoother although still slightly asymmetric. The calculation for the donor-aryl-sulfur molecule (figure 3(e)) proved problematic to converge at larger bias and the features observed beyond 2 V positive or negative bias are most likely not real features. This curve has been included for completeness.

To explain some of the features observed in the calculated $i(V)$ curves, an examination of the molecular orbital structure is illustrative. Considering first the D–C_4H_8–A molecule, conduction in the forward bias direction shows a step-like increase at an applied bias of about 1 eV. The origin of this feature is related to the molecular orbitals close to the Fermi level and their evolution relative to the electrochemical potential of the two electrodes as the bias is increased. This relationship is shown in figure 4 for both negative and positive applied bias. The highest occupied (HOMO) and lowest unoccupied molecular orbital (LUMO) are eigenvalues of the molecular-projected self-consistent Hamiltonian: this is the self-consistent Hamiltonian of the central molecule in the presence of the Au electrodes and Au surface layers. This is a convenient analysis method for projecting out the electrodes and surface atoms [26]. It should be noted that the reference

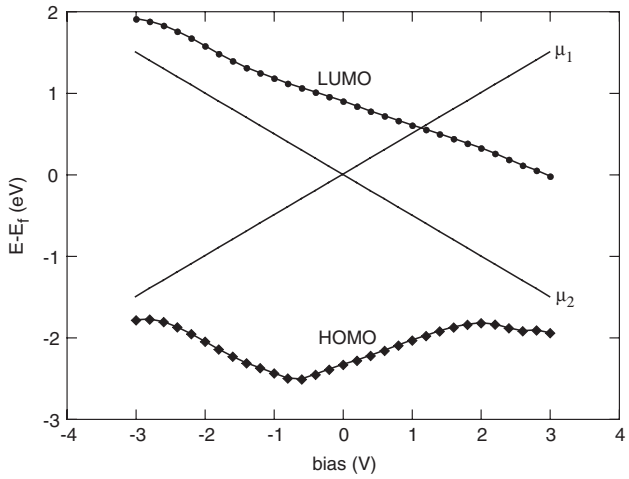

Figure 4. Orbital energies of the HOMO and LUMO level for the D–C_4H_8–A molecule as a function of applied bias. The two solid lines show the electrochemical potential of the left (μ_1) and right (μ_2) electrodes.

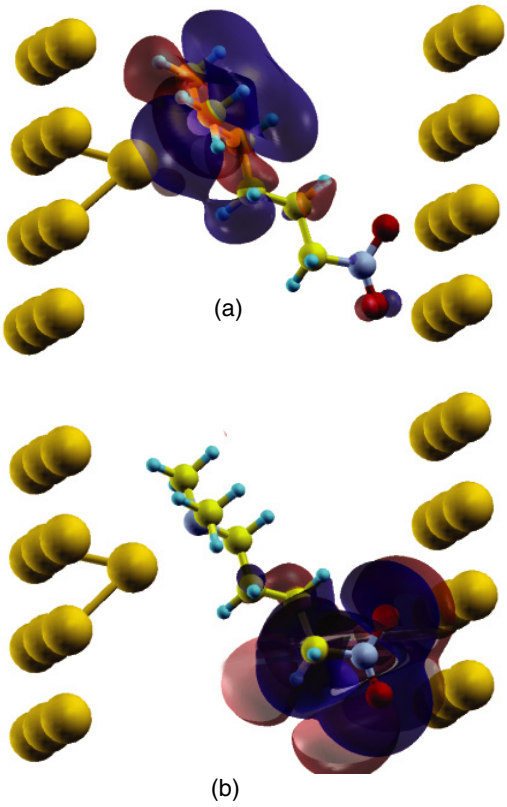

Figure 5. Probability isosurfaces for the (a) HOMO and (b) LUMO of the D–C_4H_8–A molecule. The isosurface value for the HOMO is twice the LUMO. Graphic generated with the XcrySDen software package [30].

energy in figure 4 is the pseudo-Fermi energy of the system, that is, the Fermi energy at zero bias. Experimentally, the electrochemical potential of one electrode is normally fixed (the source electrode) while that of the other electrode is varied, causing the pseudo-Fermi energy to vary with it.

The HOMO, as expected, is the donor level and is located predominantly on the methyl endgroup closest to the left electrode. The LUMO is the acceptor level and associated with the nitro group attached to the right electrode. This is illustrated in the diagrams of these orbitals shown in figure 5 where probability isosurfaces are plotted for each orbital at values of 0.005 and 0.01 for the LUMO and HOMO, respectively. Again, these orbitals are the eigenfunctions of the molecular-projected self-consistent Hamiltonian.

For positive bias, the electrochemical potential of the right electrode lies below the left electrode and there will be a tendency for electrons to travel from left to right to bring the two electrodes into equilibrium. At a bias of +1.0 V, the energy of the LUMO crosses the electrochemical potential of the opposite electrode and falls into the bias window. An electron can now tunnel into this level directly from the left electrode and escape into the right electrode, giving a rise in the current. The HOMO level remains well below the electrochemical potential of the right electrode and energy of the LUMO and so electrons cannot tunnel from this level at an applied bias of up to +3.0 V. It is interesting that the energy of the LUMO follows the electrochemical potential of the electrode it is connected to, while the energy of the HOMO remains relatively stationary. This might suggest that the acceptor end of the molecule is more strongly coupled to its electrode, despite the presence of the Au adatom on the donor side of the molecule.

The position of the LUMO relative to the electrochemical potential of the electrodes for the other two donor–bridge–acceptor molecules shows the same trend, giving rise to similar behaviour in the positive quadrants of the $i(V)$ curves. For the D–C_8H_{16}–A molecule, the tunnel length is considerably longer as the bridge section of the molecule is now approximately twice as long and consequently the current decreases by an order of magnitude. Replacing the bridge with a 1,4-substituted benzene ring, i.e. a C_6H_4 group, gives rise to more delocalized orbitals. In particular, the HOMO extends across the molecule and hence the current increases by an order of magnitude compared to the butane bridged molecule. The HOMO and LUMO isosurfaces are shown in figure 6.

In the original Aviram and Ratner calculations [1] the conductance in this bias direction is suppressed almost completely, presumably because the acceptor level does not cross into the bias window and always lies above the electrochemical potential of the right electrode.

For reverse bias the HOMO and LUMO energies trend towards the electrochemical potential of their respective electrodes. In this regime the tendency is for electrons to travel from right to left in order to bring the electrochemical potentials of the electrodes into equilibrium. Aviram and Ratner calculate large current flow in this regime once the turn-on voltage is passed. The mechanism they propose is that the acceptor levels overlap the occupied levels in the nearest electrode and an electron can therefore tunnel from the electrode onto the acceptor level. Similarly an electron can tunnel from the donor level on the opposite end of the molecule to the respective electrode. There is now an additional electron on the acceptor end of the molecule and hole on the donor end. This electron can tunnel across the bridge portion of the molecule into the donor level. Because the acceptor level

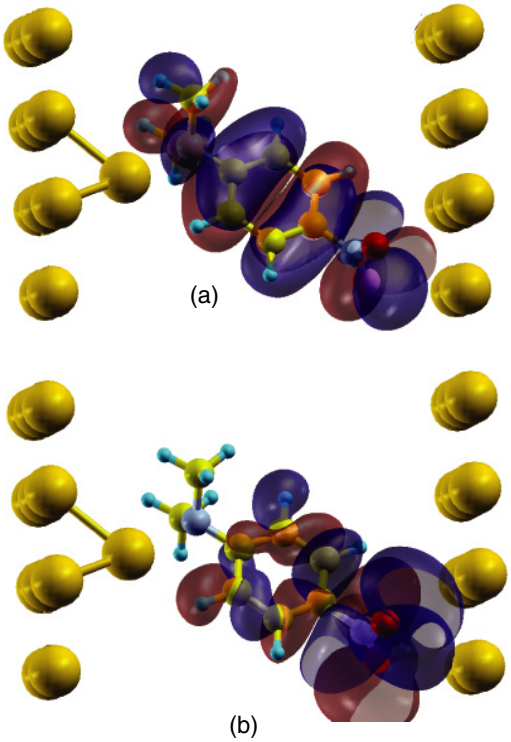

Figure 6. Probability isosurfaces for the (a) HOMO and (b) LUMO of the D–C_6H_4–A molecule. The isosurface value for the HOMO is twice the LUMO. Graphic generated with the XcrySDen software package [30].

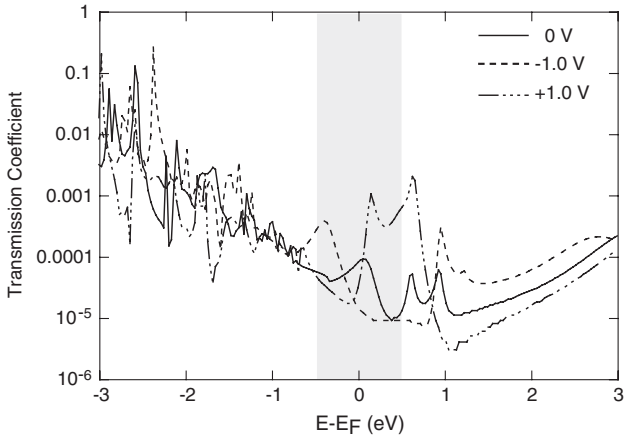

Figure 7. Transmission spectra for D–C_4H_8–A calculated at zero and finite bias. The shaded region shows the bias window at ±1.0 V.

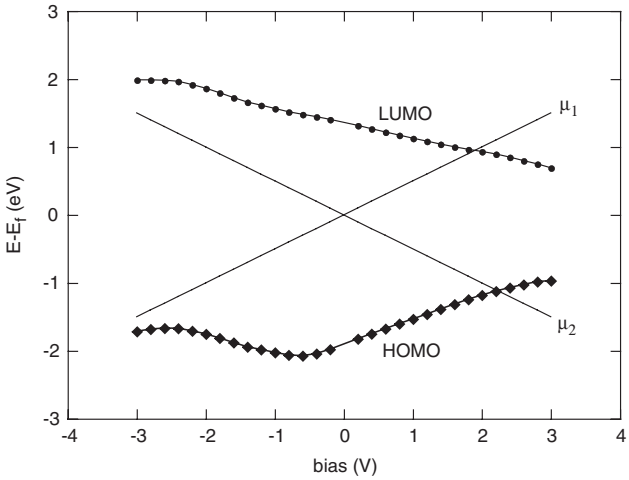

Figure 8. Orbital energies of the HOMO and LUMO level for the S–C_4H_8–A molecule as a function of applied bias. The two solid lines show the electrochemical potential of the left (μ_1) and right (μ_2) electrodes.

lies above the donor level in energy the electron tunnels into an excited Franck–Condon state and subsequently undergoes a radiationless decay. This process is blocked in the opposite direction giving a rectifying behaviour. A similar model would explain the relatively large currents observed under reverse bias in the present case. Although we use the same current and voltage sign convention as Aviram and Ratner, the molecules presented here are oriented in the opposite direction. At a bias of −2.5 V the energy of the HOMO level is now close to the electrochemical potential of the left electrode and electrons can tunnel easily from this level into the unoccupied states of the left electrode. At smaller bias the HOMO energy is far removed from the left electrochemical potential and the current is suppressed, hence the current under reverse bias begins to increase rapidly at around a bias of −2.5 V.

A similar argument may be applied to the D–C_8H_{16}–A and D–C_6H_4–A molecules under reverse bias: however, tunnelling across the central bridge portion of the molecule is modified either by the length of the bridge or delocalization of the orbitals.

The transmission spectra for the D–C_4H_8–A molecule at zero, positive and negative bias shown in figure 7 provide more detail for the features in the positive quadrant of figure 3(a).

There are two peaks at approximately 1 eV above the Fermi energy at 0 V bias; these are the LUMO and LUMO + 1. As the bias becomes more positive these peaks move towards the Fermi level and the current increases as the first peak moves into the bias window at about +0.5 V. At +1.0 V the second peak moves into the bias window and the current again increases. For negative bias these peaks move away from the Fermi level, and at −1.0 V there are now large peaks within the bias window giving only a small current. This is consistent with the data in figure 4.

Figure 8 shows the evolution of the HOMO and LUMO level for the S–C_4H_8–A molecule. Here, the donor group has been replaced by a less electron-donating sulfur group, which now produces the HOMO level. At sufficient positive bias (about +2.0 V) both the HOMO and LUMO orbitals cross into the bias window, although there is no obvious increase in the current at this point in figure 3(d). Furthermore the $i(V)$ curve for this molecule is more symmetric compared with the corresponding donor–bridge–acceptor molecule. This could be a consequence of the strong interaction between the terminal sulfur and adjacent gold electrode which tends to couple the molecule to the electrode more effectively. The binding energies for the amine moiety to gold surfaces are of the order of 0.5 eV [22], whereas sulfur–gold bonds in thiol moieties are of the order of 2 eV [24]. Larger currents and a

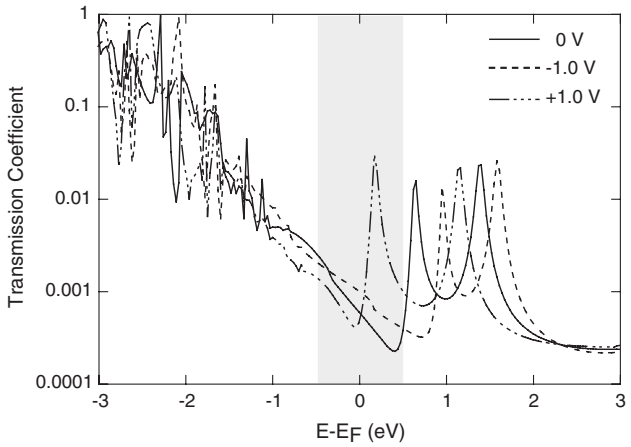

Figure 9. Transmission spectra for S–C_4H_8–A calculated at zero and finite bias. The shaded region shows the bias window at ±1.0 V.

smoother, more symmetric $i(V)$ curve is also observed for the S–C_6H_4–A molecule.

So far the position of the HOMO and LUMO relative to the bias window have been considered: however, the width of these levels will also influence the $i(V)$ characteristic. Broadening of the molecular energy levels is associated with interaction with the gold electrodes. As the binding energy increases certain molecular levels become broader due to hybridization with the gold orbitals. Broader energy levels can enter the bias window at lower bias values and hence give rise to larger currents. It is unlikely, however, that this is the main reason for the increased current upon substituting a sulfur linkage for the amine group in the D–C_4H_8–A molecule. In both molecules the LUMO level plays a significant role in the transport process, as figures 4 and 8 indicate. These levels are associated with the nitro (acceptor) group whereas the sulfur atom on the other end of the S–C_4H_8–A molecule participates in the strong bond with the Au surface. Figure 9 shows the transmission spectra for the S–C_4H_8–A molecule at 0, −1 and +1 V bias. There are two obvious resonances above the Fermi energy associated with the LUMO and LUMO + 1 orbitals on the acceptor group, analogous to the D–C_4H_8–A molecule. The two resonances are split further apart than in the D–C_4H_8–A molecule with the LUMO resonance at about the same energy. The width of the resonances does not appear to be influenced by the stronger binding energy of the sulfur atom in S–C_4H_8–A. The transmission coefficient in the region of these resonances is an order of magnitude larger for the S–C_4H_8–A molecule, however. Rather than broadening the energy levels this might suggest the stronger link to the Au surface increases the overall magnitude of the transmission coefficient, even though the orbitals associated with this coupling to the electrode do participate directly in the transport process.

4. Conclusions

Electron transport through a series of molecular junctions has been calculated using the density functional theory (DFT) combined with a non-equilibrium Green's function (NEGF) approach. The molecules are simple examples of the type proposed by Aviram and Ratner in their original 1974 paper [1] where a donor and acceptor group are linked by a central bridge molecule. In the present case the donor and acceptor are the dimethylamino and nitro moieties, respectively. The bridges considered are butane, octane and substituted benzene groups.

The calculated current is modified by the nature of the bridge in a manner that is quite intuitive and not surprising. Doubling the length of the alkane bridge decreases the current by an order of magnitude, as expected since the central tunnelling region is now twice as long. Replacing the bridge with an aryl moiety increases the current by an order of magnitude due to the relatively delocalized molecular orbitals.

More significant is the observation of an anomalous rectifying behaviour at low applied bias. We observe rectifying behaviour, or more precisely an asymmetry in the $i(V)$ curve, in the same direction as Aviram and Ratner only at high bias voltages in excess of ±2.5 V. Moreover, the effect is rather weak with rectification ratios limited to about a factor of 2. In this region the larger current occurs for positive bias at the acceptor end of the molecule. This result can be interpreted in terms of transfer of electrons from the electrode onto the acceptor, tunnelling across the bridge onto the ionized donor and finally tunnelling into the adjacent electrode. For smaller applied bias, up to about ±2.5 V, there is an asymmetry in the opposite direction. This is attributed to the LUMO level of the acceptor group which crosses into the bias window at about +1.0 V. Electrons can now tunnel from the opposite electrode directly into this unoccupied level and consequently onto the adjacent electrode.

In the context of molecular electronics these results show that only modest rectification can be achieved in these donor–acceptor molecules for voltage ranges of the order of a few volts. Although the $i(V)$ curves are quite asymmetric in shape overall, the anomalous rectification at small bias limits the overall rectification to about a factor of two at higher positive and negative bias. At lower applied bias where this anomalous rectification dominates, the ratio of reverse to forward bias current is slightly larger and reaches a maximum value of approximately 4 at about 1 V. More importantly, the rectification will switch direction for input levels that cross ±2.5 V, meaning the response of the device would not be a simple rectification of an input alternating signal. There may, of course, be situations in which this behaviour can be used to benefit.

Acknowledgments

This work was supported by the Australian Research Council. High performance computing facilities were provided under the merit allocation schemes of ac3 (in NSW) and the National Facility, APAC.

References

[1] Aviram A and Ratner M A 1974 *Chem. Phys. Lett.* **29** 277–83
[2] Martin A S, Sambles J R and Ashwell G J 1993 *Phys. Rev. Lett.* **70** 218–21

[3] Metzger R M *et al* 1997 *J. Am. Chem. Soc.* **119** 10455–66
[4] Heath J R and Ratner M A 2003 *Phys. Today* **56** 43–9
[5] Joachim C and Ratner M A 2005 *Proc. Natl Acad. Sci. USA* **102** 8801–8
[6] Adams D M *et al* 2003 *J. Phys. Chem.* B **107** 6668
[7] James D K and Tour J M 2004 *Chem. Mater.* **16** 4423–35
[8] Stokbro K, Taylor J and Brandbyge M 2003 *J. Am. Chem. Soc.* **125** 3674–5
[9] Ellenbogen J C and Love J C 2000 *Proc. IEEE* **88** 386
[10] Datta S 2005 *Quantum Transport: Atom to Transistor* (Cambridge: Cambridge University Press)
[11] Armstrong N, Hoft R C, McDonagh A, Cortie M B and Ford M J 2007 *Nano Lett.* **7** 3018
[12] Soler J M, Artacho E, Gale J D, Garcia A, Junquera J, Ordejon P and Sanchez-Portal D 2002 *J. Phys.: Condens. Matter* **14** 2745–79
[13] Ordejon P, Artacho E and Soler J M 1996 *Phys. Rev.* B **53** 10441–4
[14] Kohn W and Sham L J 1965 *Phys. Rev.* **140** A1133–8
[15] Hohenberg P and Kohn W 1964 *Phys. Rev.* **136** B864–71
[16] Perdew J P, Burke K and Ernzerhof M 1996 *Phys. Rev. Lett.* **77** 3865–8
[17] Ford M J, Hoft R C and McDonagh A 2005 *J. Phys. Chem.* B **109** 20387–92
[18] Hoft R C, Armstrong N, Ford M and Cortie M B 2007 *J. Phys.: Condens. Matter* **19** 215206
[19] Hoft R C, Ford M J and Cortie M B 2007 *Mol. Simul.* **33** 897
[20] Troullier N and Martins J L 1991 *Phys. Rev.* B **43** 1993–2006
[21] Johnson D D 1988 *Phys. Rev.* B **38** 12807
[22] Hoft R C, Ford M J, McDonagh A and Cortie M B 2007 *J. Phys. Chem.* C **111** 13886
[23] Venkataraman L, Klare J E, Tam I W, Nuckolls C, Hybertsen M S and Steigerwald M L 2006 *Nano Lett.* **6** 458–62
[24] Ford M J, Hoft R C and Gale J D 2006 *Mol. Simul.* **32** 1219–25
[25] Monkhorst H J and Pack J D 1976 *Phys. Rev.* B **13** 5188–91
[26] Brandbyge M, Mozos J L, Ordejon P, Taylor J and Stokbro K 2002 *Phys. Rev.* B **65** 165401
[27] Muller K H 2006 *Phys. Rev.* B **73** 045403
[28] Hu Y B, Zhu Y, Gao H J and Guo H 2005 *Phys. Rev. Lett.* **95** 156803
[29] Basch H, Cohen R and Ratner M A 2005 *Nano Lett.* **5** 1668–75
[30] Kokalj A 2003 *Comput. Mater. Sci.* **28** 155 code available from http://www.xcrysden.org/